



ELSEVIER

Contents lists available at ScienceDirect

Deep-Sea Research II

journal homepage: www.elsevier.com/locate/dsr2

The inhibition of N₂O production by ocean acidification in cold temperate and polar waters

Andrew P. Rees^{a,*}, Ian J. Brown^a, Amal Jayakumar^b, Bess B. Ward^b

^a Plymouth Marine Laboratory, Prospect Place, The Hoe, Plymouth PL1 3DH, UK

^b Department of Geosciences, Guyot Hall, Princeton University, Princeton, NJ 08544, United States

ARTICLE INFO

Keywords:

Ocean acidification
Nitrous oxide
Ammonia oxidising archaea
Ammonia
Atlantic
Arctic
Antarctic

ABSTRACT

The effects of ocean acidification (OA) on nitrous oxide (N₂O) production and on the community composition of ammonium oxidizing archaea (AOA) were examined in the northern and southern sub-polar and polar Atlantic Ocean. Two research cruises were performed during June 2012 between the North Sea and Arctic Greenland and Barent Seas, and in January–February 2013 to the Antarctic Scotia Sea. Seven stations were occupied in all during which shipboard experimental manipulations of the carbonate chemistry were performed through additions of NaHCO₃⁻ + HCl in order to examine the impact of short-term (48 h for N₂O and between 96 and 168 h for AOA) exposure to control and elevated conditions of OA. During each experiment, triplicate incubations were performed at ambient conditions and at 3 lowered levels of pH which varied between 0.06 and 0.4 units according to the total scale and which were targeted at CO₂ partial pressures of ~500, 750 and 1000 μatm. The AOA assemblage in both Arctic and Antarctic regions was dominated by two major archetypes that represent the marine AOA clades most often detected in seawater. There were no significant changes in AOA assemblage composition between the beginning and end of the incubation experiments. N₂O production was sensitive to decreasing pH_T at all stations and decreased by between 2.4% and 44% with reduced pH_T values of between 0.06 and 0.4. The reduction in N₂O yield from nitrification was directly related to a decrease of between 28% and 67% in available NH₃ as a result of the pH driven shift in the NH₃:NH₄⁺ equilibrium. The maximum reduction in N₂O production at conditions projected for the end of the 21st century was estimated to be 0.82 Tg N y⁻¹.

Crown Copyright © 2015 Published by Elsevier Ltd. This is an open access article under the CC BY license (<http://creativecommons.org/licenses/by/4.0/>).

1. Introduction

Anthropogenic activities currently add 10 PgC per year to the atmosphere as CO₂. The change in atmospheric CO₂ from ~280 ppm (ppm) in pre-industrial times to 395 ppm in 2013 (Le Quéré et al., 2014) has impacted the earth system on several scales. The oceans and atmosphere are intimately linked so that changes to the partial pressure of atmospheric CO₂ result in proportional changes in dissolved CO₂ in the marine environment. As a result of this, the rise of global temperatures due to an enhanced greenhouse effect has been buffered by the exchange of approximately 25% of anthropogenic CO₂ into the oceans (Le Quéré et al., 2014) and it is this condition that has resulted in a profound change to ocean carbonate chemistry and the phenomenon of ocean acidification (OA) (Raven et al., 2005). As a consequence pH has decreased by 0.0011–0.0024 units per year for the last two

decades (Rhein et al., 2013), so that oceanic pH is on average ~0.1 units lower than it was prior to the industrial revolution. This pH decrease equates to an increase in acidity of 26% and further increases are predicted. Projections afforded by the current generation (CMIP5) of model-based scenarios (Moss et al., 2010) indicate decreasing ocean pH of between 0.06 and 0.33 units for the 2090s relative to the 1990s for “high mitigation” RCP2.6 and the “business as usual” RCP8.5 scenarios respectively (Bopp et al., 2013; Ciais et al., 2013). Based on our current understanding of microbial biogeochemistry, it is expected that elevated oceanic pCO₂ and the subsequent decrease in pH will have direct (e.g. the increase in N₂ and CO₂ fixation by *Trichodesmium*; Hutchins et al., 2007) and indirect (e.g. the increase in shallow water remineralisation associated with a reduced ballast effect; Hofmann and Schellnhuber, 2009) impacts on microbial nutrient cycling. It is considered that these effects may fundamentally alter current biogeochemical cycles (e.g. Codispoti, 2010).

N₂O is a trace gas whose atmospheric concentration is increasing at a mean rate of ~0.75 ppb yr⁻¹ (Hartmann et al.,

* Corresponding author.

E-mail address: apre@pml.ac.uk (A.P. Rees).

2013). It is a greenhouse gas with a global warming potential on a 100 year timescale of approximately 300 times that of CO₂ (Ramaswamy et al., 2001) and it contributes significantly to stratospheric ozone depletion (Ravishankara et al., 2009). Though the N₂O concentration in most of the surface of the global ocean is in close equilibrium with the atmosphere (Nevison et al., 1995), the oceans contribute about 30% of the natural N₂O source to the atmosphere (Bange, 2006) and there is a fine balance between the oceans acting as net producer or consumer of N₂O. Environmental effects associated with a changing climate, which include rising temperatures, oxygen depletion and ocean acidification are quite likely to impact the level of this equilibrium (Codispoti, 2010).

Nitrous oxide is biologically produced through three processes: nitrification involves the two stage aerobic oxidation of NH₄⁺ through NO₂⁻ to NO₃⁻, where the release of N₂O as a by-product is dependent on the ambient O₂ concentration (Goreau et al., 1980; Loescher et al., 2012). Denitrification is the anaerobic transformation of NO₃⁻ into N₂ which has N₂O as an intermediate. In the third route, nitrifier-denitrification, N₂O can be formed during the reduction of NO₂⁻ via nitric oxide to N₂O. In the open oceans nitrification is the dominant mechanism for the production of N₂O (Freing et al., 2012), and in the limited number of studies that have been reported, this process has been shown to be particularly sensitive to OA in sub-surface marine waters. Huesemann et al. (2002) found a linear reduction in nitrification rate with high additions of CO₂, so that at pH 6.5, nitrification was reduced by up to 90% of the natural condition. That experiment was more relevant to the effects associated with CO₂ disposal than with levels of OA predicted for the coming century. In a study where pH was manipulated between 8.09 and 7.42 at several locations in the Pacific and Atlantic, Beman et al. (2011) showed unequivocal evidence for an inhibitory effect of short term OA on nitrification. Kitidis et al. (2011) manipulated conditions of pH between ambient and 6.5 for water column samples from the English Channel and found that ammonium oxidation rate decreased with decreasing pH to near complete inhibition at pH 6.5.

It has been hypothesized that nitrification rates may be altered by increasing OA either directly, by impacting on microbial physiology or community composition, or indirectly by changes to the supply of organic material (Codispoti, 2010). Hutchins et al. (2009) speculated that increasing levels of CO₂ may lead to an increase in autotrophic nitrification rates through a reduction of CO₂ limitation or CO₂ fertilization effect. To date this effect has not been observed for the open ocean and the limited number of studies have shown some equivocality in their findings. Clark et al. (2014) performed an investigation of OA on nitrification and N₂O in near surface (~5 m) waters of the NW European shelf seas. The absence of any relationship between OA and N₂O observed is, in part, attributed to the oxygenated status of these waters and the low production of N₂O expected. Clark et al. also observed variability in the impact of OA on nitrification which did not allow a relationship or mechanistic understanding of the relationship between OA and nitrification to be developed. In a study of estuarine and near coastal waters of Narragansett Bay, Fulweiler et al. (2011) found that nitrification rates increased along decreasing natural gradients of pH. Whilst not dismissing the CO₂ fertilisation effect, Fulweiler et al. concluded that a combination of environmental conditions was likely to be the biggest driver influencing nitrification. The decrease in rates could be associated with change in the microbial community possibly as a result of competitive strength to compete for available NH₄⁺/NH₃, or as a result of reduced NH₃, the favored substrate for the first stage of nitrification (Ward, 2008a). The NH₄⁺:NH₃ equilibrium has a *pK_a* of ~9.2, favouring NH₄⁺ in an acidifying ocean.

Changes in the microbial ammonium oxidising community composition as a result of changing OA have been reported by

Bowen et al. (2013) who saw greater changes in assemblage composition and abundance of ammonium oxidising bacteria (AOB) than of ammonium oxidising archaea (AOA). Whilst both AOB and AOA are found throughout the oceans and produce N₂O (Santoro et al., 2011; Loescher et al., 2012) AOA are considered to be the principal nitrifying organisms (Wuchter et al., 2006).

To our knowledge, there are no reports to date which confirm the inhibition of N₂O production by OA, although the limited evidence from studies on nitrification indicate that this is to be expected. Decreasing oceanic oxygen and decreasing ballast effect (sinking rate of particles) are both predicted to increase the release of N₂O from nitrification in a future ocean (Codispoti, 2010; Gehlen et al., 2011) and so prediction of the overall N₂O inventory and net emissions will prove problematic. Beman et al. (2011) performed an indicative budget for N₂O production from nitrification, which suggested that a decrease in nitrification between 3% and 44% (the range indicated by Beman for the next 20 to 30 years) could result in reduced N₂O emissions comparable to all current N₂O production from fossil fuel combustion and industrial processes.

Here we report on two studies (Tyrrell et al., this issue) performed to investigate the impact of OA on N₂O production and AOA distribution as a contribution to the United Kingdom Ocean Acidification (UKOA) program. Experiments were performed at ocean stations (E01–E05) during cruise JR271 of the RRS James Clark Ross between the North Sea and Arctic Ocean in June 2012, and at stations (B03 and B04) during cruise JR274 to the Southern Ocean in January–February 2013 (Fig. 1).

2. Methods

Seawater was collected from Niskin bottles deployed on a titanium frame at the base of the surface mixed-layer defined by the temperature profile (except for E04). The Niskin bottles were transferred to a positive pressure Class-100 filtered trace metal clean container to avoid contamination. Unfiltered water was dispensed into 4.5 L polycarbonate incubation bottles and the bottles were closed pending carbonate chemistry manipulation. Single experimental bottles were individually manipulated to achieve a range of 4 different target pCO₂ levels (ambient, 550, 750 and 1000 μatm), according to the initial carbonate chemistry of the seawater at the time of the water collection. The manipulation of the carbonate system was achieved through additions of NaHCO₃⁻ + HCl (Borowitzka, 1981; Gattuso and Lavigne, 2009; Schulz et al., 2009) and immediately verified by total alkalinity (TA) and DIC analyses. Values of pCO₂ and pH_T (total scale) were determined using CO2sys (Lewis and Wallace, 1998). Following manipulation of pCO₂, bottles were closed with PTFE backed butyl septa before being further sealed with parafilm and incubated.

Tests have been performed previously to confirm the validity of this approach and to test the integrity of the polycarbonate bottles to N₂O diffusion. At six positions on a transect through the Atlantic Ocean between the UK and the Falkland Islands, replicate bottles (2–4) were filled with seawater and poisoned with the addition of 1 ml saturated HgCl₂ and incubated in the dark at collection temperature. N₂O concentration was determined on collection, and thereafter triplicate analyses of N₂O were made at several time points over 6 days. N₂O concentration remained stable during each of these storage tests, the coefficient of variation varied between 1.3% and 5.2% (mean 3.9%, *n* = 16 time points × 3 analyses). *F* tests between N₂O in killed samples and initial concentrations, and between killed samples and the expected (atmospheric equilibrium) concentration confirmed 86% and 87% similarity in variance respectively.

During this study, N₂O concentration was determined in triplicate on samples first prepared (T0) and after 48 h (T48) of

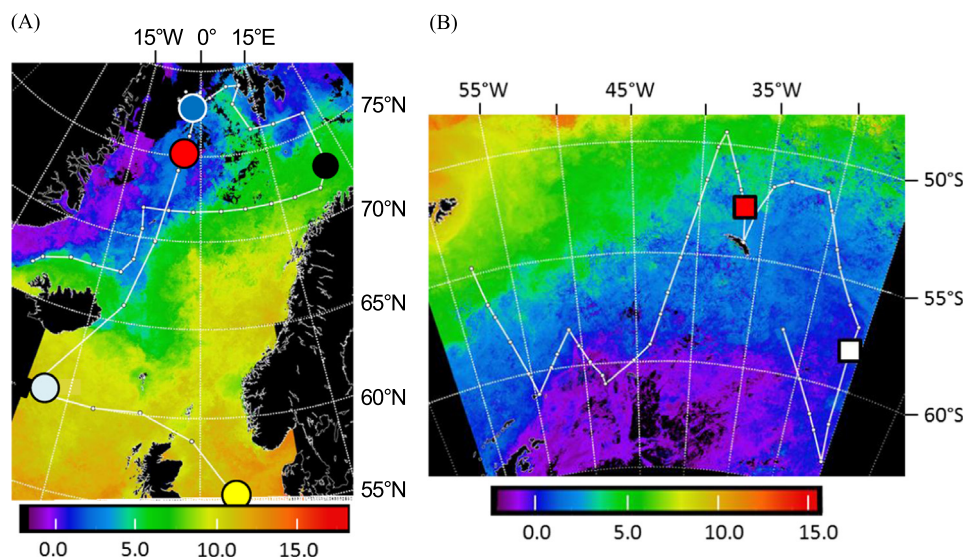


Fig. 1. Location of experiments performed during (a) JR271 in June 2012 and (b) JR274 in January–February 2013.

incubation. Subsamples from the incubations were filtered for determination of AOA at T0 and at several time points afterwards. Incubations were performed in the dark within a purpose-built experimental laboratory container allowing precise temperature control. The temperature was adjusted to the in situ value at the time of the water collection. Temperature within a dummy incubation bottle was monitored using a traceable thermometer, while two recording thermometers were used to monitor air temperature in the incubator. Samples were also collected for N₂O analysis from CTD casts performed at each of the experimental stations during JR271 only.

2.1. N₂O analysis

Samples were collected using acid cleaned Tygon tubing directly from CTD Niskin bottles or by siphoning from 4.5 L incubation bottles into 1 L borosilicate flasks. Single samples were taken from CTD bottles and triplicates from the incubated sample. Samples were overfilled in order to expel air bubbles, poisoned with 200 μ L of saturated HgCl₂ solution and temperature equilibrated at 25.0 ± 0.5 °C. In all cases samples were analyzed within 8 h of collection. N₂O was determined by single-phase equilibration gas chromatography with electron capture detection similar to that described by Upstill-Goddard et al. (1996). Each individual sample was calibrated against three certified ($\pm 5\%$) reference standards of 287, 402 and 511 ppb (Air Products Ltd.) which are traceable to NOAA WMO-N2O-X2006A scale for N₂O mole fractions. Mean instrument precision from daily, triplicate analyses of the three calibration standards ($n=81$) was 0.95%. Concentrations of N₂O in seawater were calculated from solubility tables of (Weiss and Price, 1980) at equilibration temperature (~ 25 °C) and salinity. All N₂O data from this study are available from the British Oceanographic Data Centre according to: <http://dx.doi.org/10.5285/268dfd3b-dcc6-3f4a-e053-6c86abc0c2f9>.

2.2. amoA AOA microarray

The array (BC016) was developed following the archetype array approach described and employed previously (e.g. Ward and Bouskill, 2011; Bowen et al., 2013), with 90-mer oligonucleotide probes. Each probe included an amoA-specific 70-mer region and a 20-mer control region (5'-GTACTACTAGCCTAGGCTAG-3') bound to a glass slide. The design and spotting of the probes have been

described previously (Bulow et al., 2008). Using an established algorithm (Bulow et al., 2008), 99 different archetypes were identified representing 8296 archaeal amoA sequences, which had been aligned and analyzed by Biller et al. (2012). The Archetype probes are numbered according to their representation in the database; of the > 8000 sequences aligned by Biller et al. (2012), the largest number of them, 1191 are represented by AOA1, 1149 by AOA2 and 795 by AOA3, and so forth. The probe accession numbers and sequences are listed in Table S1.

2.3. Target preparation, microarray hybridization, and data analysis

Seawater samples (up to 8 L) were filtered onto 0.2 μ m pore size Sterivex filters (Millipore, Billerica, MA) using a peristaltic pump, and filters were flash frozen in liquid nitrogen and stored at -80 °C. Total DNA and RNA were extracted from Sterivex filters using the AllPrep DNA/RNA Kit (Qiagen Sciences) with slight modifications (as in Ward, 2008b) to the manufacturer's instructions. The extraction procedures were performed twice on each Sterivex filter in order to maximize the DNA yield. cDNA was made from the RNA immediately upon purification using the Superscript III Kit (Life Technologies) following the manufacturer's instructions after concentrating the RNA extract using MinElute columns (Qiagen Sciences).

Archaeal amoA genes were amplified from the DNA and cDNA using primers Arch-amoAF (5'-STAATGGTCTGGCTTAGACG-3') and Arch-amoAR (5'-GCGCCATCCATCTGTATGT-3') and protocols as described by Francis et al. (2005). DNA and cDNA from To and Tf (Tf=T final=96 h for all five Arctic experiments, 144 h for Antarctic experiment B03 and 168 h for Antarctic experiment B04). Targets for microarray hybridization were prepared from the amoA PCR products according to Ward and Bouskill (2011), hybridized in duplicate on a microarray slide and washed as described previously (Ward and Bouskill, 2011). Washed slides were scanned using a laser scanner 4300 (Agilent Technologies, Palo Alto, CA) and analyzed with GenePix Pro 6.0 (Molecular Devices, Sunnyvale, CA). Quantification of hybridization signals was performed as described previously (Ward and Bouskill, 2011). A normalized fluorescence ratio (FRn) for each archetype was calculated by dividing the fluorescence signal of the archetype by the highest fluorescence signal within the same array. Then the FRn of each archetype from the duplicate arrays were averaged. The relative fluorescence ratio (RFR) of each archetype was calculated as the

contribution of FRn of the archetype to the sum of FRn of all *amoA* archetypes on the array and averaged for duplicate arrays from each sample. The original array data are available at Gene Expression Omnibus (<http://www.ncbi.nlm.nih.gov/projects/geo/>) at the National Center for Biotechnology Information under GEO Accession no. GSE72072.

2.4. Statistical analysis

The array data were analyzed using the *vegan* package in R (CRAN website; <http://www.R-project.org/>) (Borcard et al., 2011). RFR values were transformed (Arcsin(Square root)) in order to normalize the proportional data. Environmental data were transformed (square root) and then standardized around zero (deco-standard in *vegan*). The transformed data were used in all diversity and ordination analyses according to Borcard et al. (2011). The null hypothesis that the *amoA* community composition did not differ between groups of samples (e.g., time points or experiments) was tested using Multi-response Permutation Procedure (MRPP) (Zimmerman et al., 1985) with a significance level of 5%.

3. Results

3.1. Station environmental characteristic

A full description of the carbonate chemistry during both cruises is presented by Tynan et al. (this issue). During cruise JR271 in the Arctic region, the range of conditions experienced ranged between the nutrient poor northern North Sea to higher surface nitrate concentrations within the sea-ice of the Fram Strait in the Greenland Sea (Table 1). Experimental stations E01 and E02 were representative of the summertime North Atlantic and can be seen to cluster closely with respect to their surface temperature and salinity signal (Fig. 2), but are distinct with regards NO_3^- , NH_4^+ and pCO_2/pH signals (Table 1). Temperature at the depth of sample collection during JR271 (Fig. 3) ranged between -1.76°C at station E04 and 9.49°C at station E02. For the 5 stations occupied during JR271, pCO_2 was maximal at E02 at 391.5 (pH minimum of 8.051) and decreased to a minimum of 263.0 μatm at E04 (maximum pH of 8.186) within the Arctic ice-fields.

Southern Ocean stations B03 and B04 during JR274 were selected primarily for the benefit of other investigations to have contrasting conditions of phytoplankton biomass, with low chlorophyll concentrations of $0.63 \mu\text{g L}^{-1}$ at B03 and higher levels of $4.19 \mu\text{g L}^{-1}$ at E04. Temperatures at the depth of sample collection were 0.89 and -1.20°C at B03 and B04 respectively (Fig. 4). The highest ambient pCO_2 and lowest pH levels out of all seven stations were experienced at B03 at 425.6 μatm and 7.999 respectively. Experimental sample collection was performed as soon as possible after arrival at the station position and before

water column profiles of N_2O could be performed. Seawater for experimental manipulation was collected from the base of the surface mixed layer, which was determined from the temperature profile, to coincide with expected maxima in near surface N_2O concentration and production from nitrification (e.g. Forster et al., 2009; Kitidis et al., 2010). During JR271 this approach proved successful at stations E01, E02, and E05 (Fig. 3a, b and e) where N_2O concentrations were elevated relative to those at the immediate surface indicative of active production at these depths. At stations E03 and E04, freshwater associated with melting ice in the near surface created a stronger defined pycnocline at approximately 38 m and 18 m respectively (inset on Fig. 3c and d) which appeared to favor nitrification and N_2O production and meant that sampling at 60 m and 40 m was of waters with reduced N_2O and apparently lower production rates.

Water column profiles of dissolved N_2O were not determined during JR274.

3.2. OA impact on N_2O concentration

Over the 48 h period of incubation N_2O was produced in all bottles which had received no amendment to their carbonate chemistry. That is, there was a mean production of N_2O of 5.9, 6.6, 1.4, 0.3 and 3.6 nmol L^{-1} in two days for stations E01–E05 respectively during JR271 and of 2.2 and 1.1 nmol L^{-1} for stations B03 and B04 respectively during JR274. In all cases the concentration of N_2O decreased linearly with increasing OA (Fig. 4, Table 2) between ambient pH and pH 7.75. The observed decrease in N_2O concentration between treatments ranged between 12.4% and 43.3% of the ambient condition during JR271. The largest changes in response to OA treatment were experienced at stations E01, E02 and E05 (37.7%, 43.3% and 23.8% respectively) where water sample collection was closest to the region of maximum

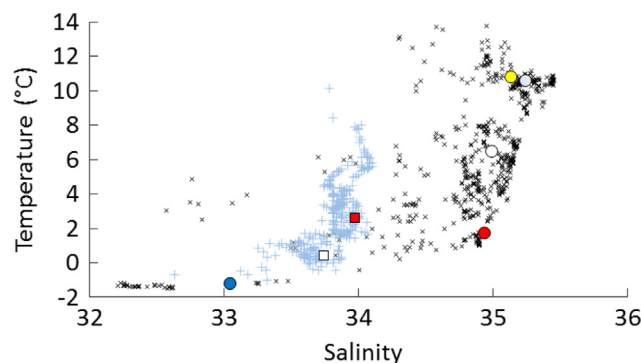


Fig. 2. Surface temperature versus salinity for cruises JR271 (X) and JR274 (+). Experimental stations are represented by E01 (●), E02 (○), E03 (●), E04 (●), E05 (●), B03 (■) and B04 (□).

Table 1

Location of ocean acidification experiments and environmental variables encountered during JR271 (June 2012) and JR274 (January–February 2013).

Experiment	Latitude	Longitude	Depth (m)	Temp ($^\circ\text{C}$)	NO_3^- (μM)	NH_4^+ (nM)	pH	pCO_2 (μatm)	Location
JR271									
E01	56.267°N	02.633°E	50	6.7	0.65	44	8.105	339.4	North Sea
E02	60.594°N	18.857°W	60	9.49	9.18	452	8.051	391.5	South of Iceland
E03	76.175°N	02.549°W	60	0.16	10.1	502	8.152	292.0	Greenland Sea
E04	78.353°N	03.664°W	40	-1.76	4.16	69	8.186	263.0	1. Ice-Edge Greenland Sea
E05	72.892°N	26.001°E	60	6.01	8.76	178	8.110	331.4	1. In-Ice Barents Sea
JR274									
B03	52.69°S	36.63°W	85	0.89	25.83		7.999	435.6	North of South Georgia
B04	58.08°S	25.93°W	46	-1.2	21.51		8.093	343.4	East of S. Sandwich Islands

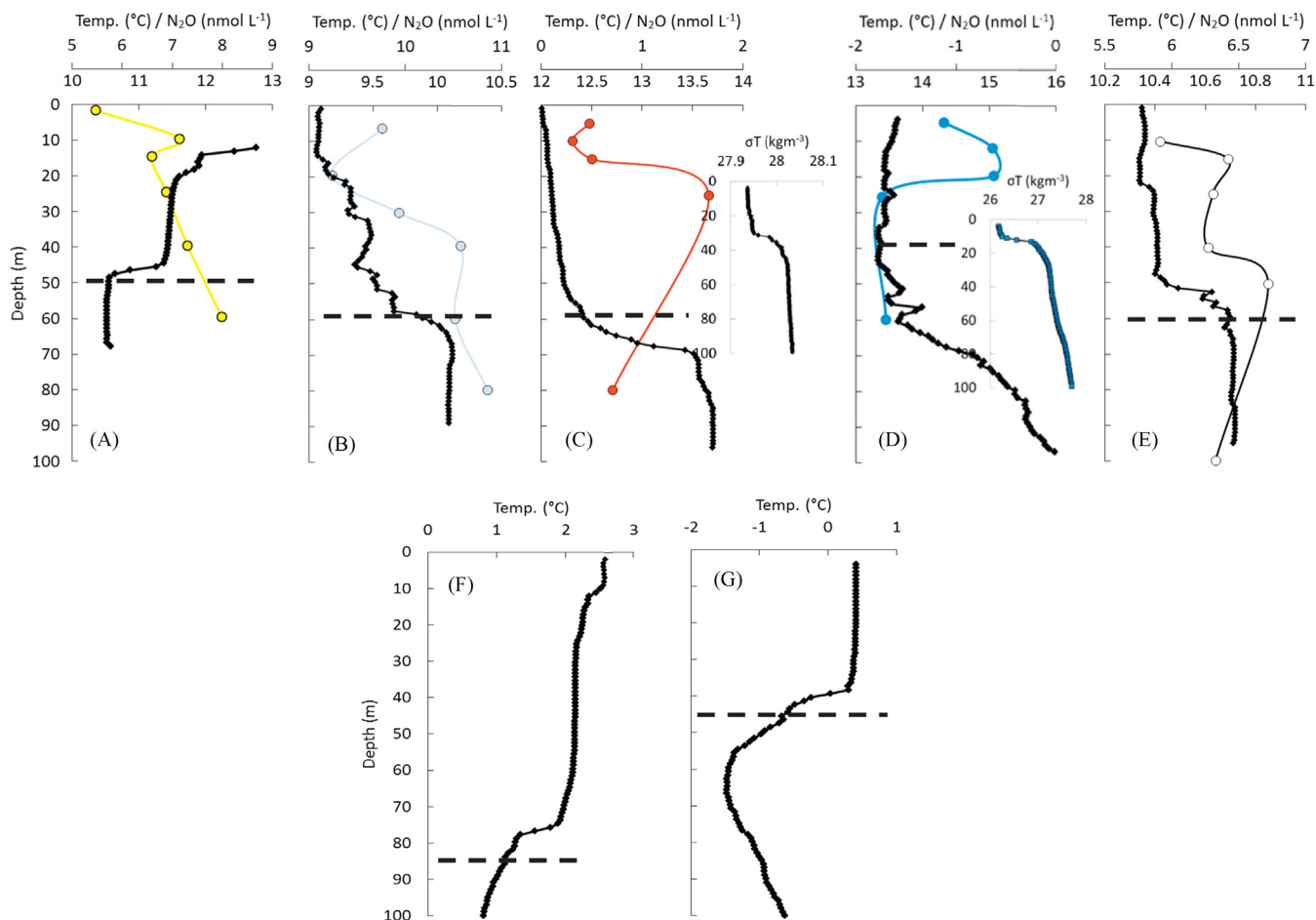


Fig. 3. Temperature and N₂O profiles for each of the experimental stations (a) E01, (b) E02, (c) E03, (d) E04, (e) E05, (f) B03, and (g) B04. In panels (c) and (d) the inset panel shows the density profile (σT). In all cases the depth of seawater sample collection is indicated by the dashed line. N₂O profiles were not performed during B03 and B04.

N₂O concentration (Fig. 3), which is assumed to be coincident with maximum production. At E03 and E04, sample water collection was approximately 35 m and 20 m below the depths of maximum N₂O, and changes in N₂O concentration with decreasing pH are less apparent (16.1% and 12.4% respectively), though still significantly correlated ($p < 0.02$). During JR274, water column profiles of N₂O were not made and so it is not possible to relate the properties of the incubated samples to the natural distribution of N₂O. Decreases in N₂O with increasing OA were observed (Fig. 4, Table 2) though these were low relative to observations during JR271 (13.1% and 4.0% for B03 and B04 respectively).

4. AOA assemblage

In the samples from the Arctic cruise JR271, 42 of the 99 archetypes were detected at 1% of the total hybridization signal in the five experiments. MRPP analysis showed that there were no significant differences in assembly composition for comparisons among stations, between To versus Tf, or between DNA versus RNA for ambient or $\sim 1000 \mu\text{atm}$. The RFR values for all samples were averaged to evaluate the relative abundance of the archetypes. Of the 42 archetypes detected at $> 1\%$ of the signal, only three had an average RFR greater than 5%. The overwhelmingly strongest signal was due to Archetype AOA3, which represents sequences from the marine water column. The second strongest signal was from Archetype AOA1, which also represents marine water column and sediment sequences, and includes the cultivated ammonia-oxidizing archaeon *Nitrosopumilus maritimus*. The third and

fourth largest RFRs were Archetypes AOA73 and AOA83, which represented only five and two sequences, respectively, in the Biller et al. (2012) database, all from sediments or soils. The RFR for the five archetypes that had the highest average signals across all samples are shown in Supplementary Fig. 1.

Consistent with the MRPP analysis, PCA clustered most of the samples together (Fig. 5). Three samples from E01, however, were distinct. DNA from 1TfAmbD and RNA from 1ToAmbR to 1Tf1000R had the greatest Archetype richness (N , number of Archetypes detected at $> 1\%$ of total signal) at 24, 17 and 15 Archetypes respectively. The next richest sample was 2Tf1000D with 13 significant Archetypes. In the other 27 samples, N ranged from 4 to 10.

Twenty-four of the 99 Archetypes were detected at 1% of the total hybridization signal in the two Antarctic experiments from JR274. The top three Archetypes were AOA3, AOA1 and AOA73 as above, but only AOA3 and AOA1 had an average RFR greater than 5%. The fourth strongest signal was AOA7, a marine water column clade representing 296 sequences in the Biller et al. (2012) database. The RFR for the five archetypes that had the highest average signals across all samples are shown in Supplementary Fig. 2.

PCA clustered the assemblages by station and between RNA and DNA (Fig. 6). MMRP analysis indicated that the assemblages in Experiments 3 and 4 were significantly different ($p < 0.004$) and that the composition of the assemblages represented in the DNA was significantly different from that in the RNA ($p < 0.013$). These differences are due to different contributions of the smaller signals; AOA1 and AOA3 were the strongest signals in all DNA and RNA samples. There were no significant differences between To

and Tf in DNA or RNA for the two experiments ($p < 0.603$). Archetype richness was greater in Experiment B04 (average $N=10.3$) than in Experiment B03 (average $N=7$) and the overall range was 4–15.

5. Discussion

The AOA assemblage in both Arctic and Antarctic regions was dominated by two major archetypes that represent the marine AOA clades most often detected in seawater. Although several other archetypes were present, the dominance of AOA1 and AOA3 implies that their physiological characteristics control the rates of

nitrification and their sensitivity to OA. The recently described oceanic AOA isolate (Santoro et al., 2015), *Candidatus Nitrosopelagicus brevis*, is a member of the AOA3 archetype, suggesting it is characteristic of the most abundant AOA in the polar oceans.

There were no significant changes in AOA assemblage composition between the beginning and end of the incubation experiments, probably because all the samples were overwhelmingly dominated by the two most abundant archetypes. The incubation period was not long enough to cause significant turnover in the assemblage, even if OA did exert differential selective pressure on the assemblage members. Significant differences were found between Antarctic stations B03 and B04, and between RNA and DNA at these stations, but not among treatments. The observed differences were due to varying relative contributions of the lower abundance archetypes and therefore imply little about the differential activity or response of the assemblage as a whole, although differential effects on N_2O production among the lower abundance archetypes cannot be ruled out. This apparent lack of sensitivity of the AOA assemblage to short term OA is consistent with the previous observation of Bowen et al. (2013) that AOA assemblages are not very sensitive to small pH changes in both long (3 weeks) and short (6 days) exposures.

Sample collection for the OA manipulation experiments was directed towards the base of the euphotic zone, and samples were

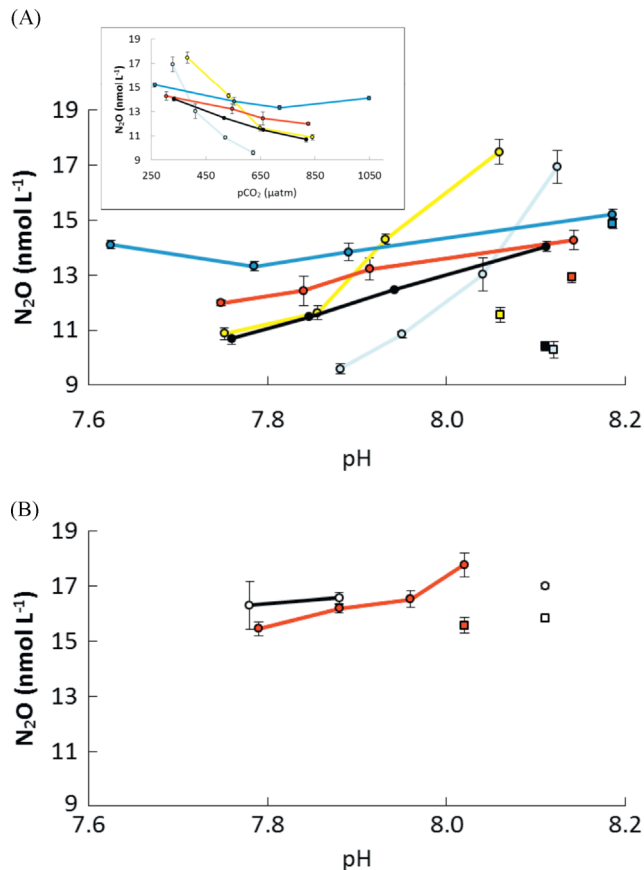


Fig. 4. Mean N_2O concentration (± 1 sd) against pH_T during CO_2 manipulation experiments during (a) JR271, with the inset showing the same N_2O data against pCO_2 , and (b) JR274. In both panels, squares represent the ambient concentration at T0, circles are N_2O concentration after 48 h incubation. In (a) E01 yellow, E02 turquoise, E03 red, E04 blue, E05 black. In panel (b) B03 red, B04 white.

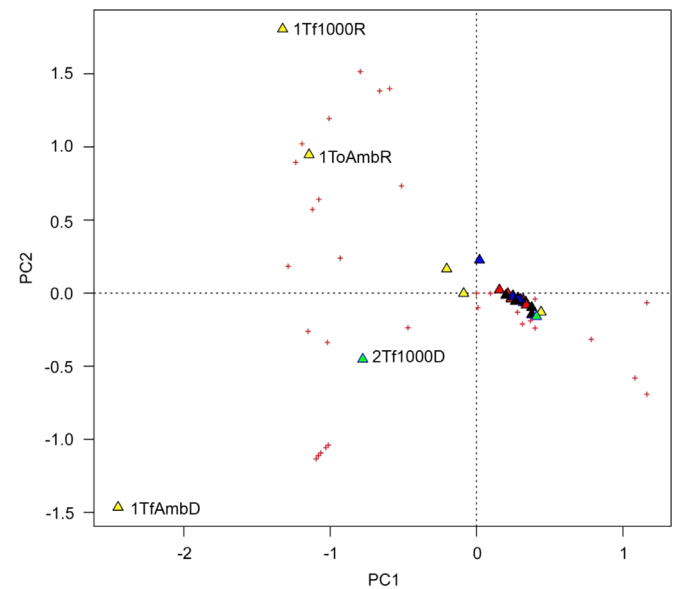


Fig. 5. PCA of AOA during JR271. Stations are color coded, E01=yellow, E02=turquoise, E03=red, E04=blue, E05=black. R=RNA (triangles); D=DNA (circles). To=initial; Tf=final. Amb=ambient; 1000=highest CO_2 treatment. Red crosses represent individual AOA archetypes.

Table 2

The linear relationship between N_2O and pH for the 7 stations occupied during JR271 and JR274.

Experiment	Ambient pH	Manipulated pH range	Regression	r^2
JR271				
E01	8.105	8.06–7.75	$N_2O = 22.44 \text{ pH} - 163.7$	0.947
E02	8.051	8.12–7.88	$N_2O = 29.721 \text{ pH} - 225.15$	0.956
E03	8.152	8.14–7.75	$N_2O = 5.8887 \text{ pH} - 33.616$	0.977
E04	8.186	8.19–7.63	$N_2O = 2.4324 \text{ pH} - 5.0328$	0.524
		8.19–7.79	$N_2O = 4.6811 \text{ pH} - 23.114$	0.999
E05	8.110	8.11–7.79	$N_2O = 9.5179 \text{ pH} - 63.166$	0.999
JR274				
B03	8.02	8.02–7.79	$N_2O = 9.2705 \text{ pH} - 56.879$	0.907
B04	8.11	8.11–7.78	$N_2O = 2.0183 \text{ pH} + 0.6177$	0.987

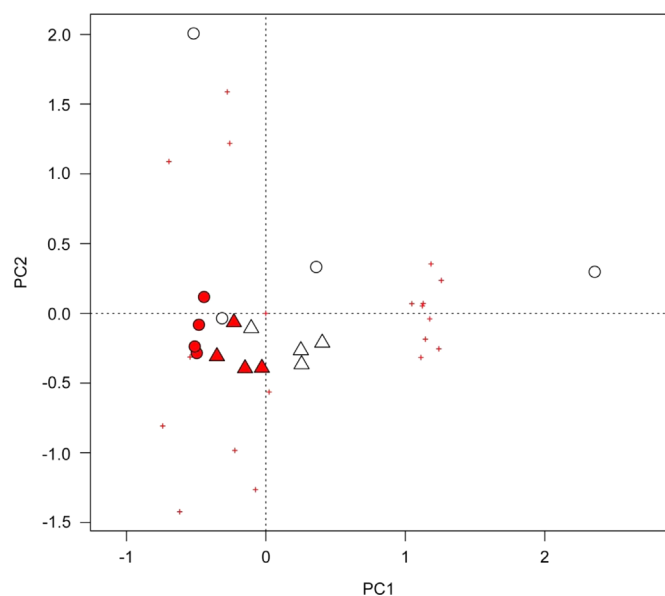


Fig. 6. PCA of AOA during JR274. Stations are color coded, B03=red, B04=white. DNA=circles; RNA=triangles. Red crosses represent individual AOA archetypes.

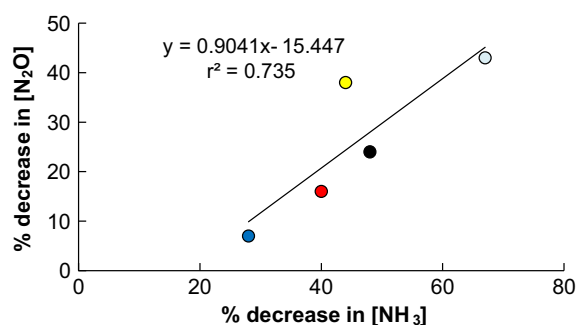


Fig. 7. Mean percentage decrease in observed N_2O concentration associated with estimated decreases in NH_3 concentration during JR271. E01 yellow, E02 turquoise, E03 red, E04 blue, E05 black.

incubated in the dark and so it is considered that competition from phytoplankton for available NH_3 or NH_4^+ is likely to be low. As the nitrifying AOA community composition proved resilient to changes in OA it would seem that observed changes in N_2O concentration were more likely associated to an altered $NH_4^+ : NH_3$ equilibrium (Hutchins et al. 2009; Beman et al., 2011). Beman et al. (2011) suggested that the decline in NH_3 with increasing OA is the driving factor in the reduced rates of NH_4^+ oxidation observed during their study. NH_3 is the substrate used in the first stage of nitrification (Ward, 2008a) and the equilibrium equations of Bell et al. (2007, 2008) indicate that at constant temperature and salinity, NH_3 concentrations in seawater would decrease by 50% over a pH change from 8.1 to 7.8 (Wyatt et al., 2010). Using the equations presented by Bell et al. we estimated concentrations of NH_3 from calculated pK_a and in-situ determined pH_T and NH_4^+ concentration. Using a fixed value of pK_a of 9.3, Beman et al. (2011) estimated that NH_3 typically represented 6.3% of total NH_x . At the stations sampled during JR271, using pK_a determined from ambient temperature and salinity (9.9, 9.9, 10.1, 10.2, 10.0 for stations E01 to E05 respectively), we estimate a mean contribution of NH_3 to NH_x of $0.68 \pm 0.15\%$. For the manipulated conditions of pH during JR271 (Table 2) the NH_3 concentration is estimated to decrease to between 28% and 67% of the ambient concentration at

the start of each experiment. Over wide geographic areas and conditions of pH or CO_2 manipulation Beman et al. (2011) found significant correlations between percentage changes in NH_3 , pH and ammonium oxidation rates, as did Huesemann et al. (2002) and Kitidis et al. (2011) between pH and ammonium oxidation. During the current study we have shown similar relationships between absolute values of pH and N_2O (Table 2) and in Fig. 7 between the percentage decrease in N_2O during incubation experiments and the decrease in NH_3 ($r^2=0.735$, $p < 0.1$) as a result of the induced shift in the $NH_4^+ : NH_3$ ratio. Our results indicate that changes in pH_T of between 0.23 and 0.4 (mean=0.31) for these ocean regions, which range between northern temperate and Arctic and Antarctic sea-ice, are likely to result in decreases of dissolved N_2O of between 12% and 43% (mean=21%), as a result of a reduced NH_3 regime of between 28% and 67%. These changes in pH_T are towards the higher end of those conditions projected for the late 21st century by CMIP5 simulations, e.g. Bopp et al. (2013) indicate decreases of 0.22 and 0.33 pH units for RCP6.0 and RCP8.5 respectively, whilst Gattuso et al. (2015) indicate a range of decrease of 0.14–0.4 pH units for RCP2.6 and RCP8.5 respectively. Both Beman et al. (2011) and Kitidis et al. (2011) observed a decline in ammonium oxidation rates even at their lowest manipulated conditions of OA. Our data confirm this sensitivity with decreases in dissolved N_2O following treatments of between 2.3% and 23% (mean=12%) at the lowest OA manipulations which varied between 0.06 and 0.23 (mean=0.13) pH units.

The decreased production of N_2O with increasing OA has the potential to offer a negative feedback to a warming environment by reducing the atmospheric radiative forcing contribution of N_2O . This could derive from two mechanisms: a direct reduction in the flux of N_2O from the ocean to the atmosphere, which could be further exacerbated by a reversal of the direction of flux, should the ocean change from source to sink of atmospheric N_2O . Beman et al. (2011) estimated that their observations of decreased nitrification rates (3–44%), would lead to a global decrease in N_2O production of between 0.06 and 0.83 $Tg N y^{-1}$ in the next 20 to 30 years. This is of particular note as it is comparable to all current N_2O production from fossil fuel combustion and industrial processes (0.7 $Tg N y^{-1}$). By taking a similar approach and assuming that 50% of the global ocean source of N_2O of 3.8 $Tg N y^{-1}$ (Denman et al., 2007) is produced through nitrification (Codispoti, 2010), the data from the current study indicate comparable, albeit slightly lower reductions in oceanic N_2O production. For the lower range of treatments (mean pH_T decrease=0.13) the estimated reduction in the ocean N_2O source is between 0.04 and 0.44 $Tg N y^{-1}$ and for the highest treatments (mean pH_T decrease=0.31) the predicted decrease ranges between 0.23 and 0.82 $Tg N y^{-1}$.

Our experiments have shown that OA will decrease the production of N_2O in the pelagic water column. It is though clearly apparent that our future oceans will not undergo OA in isolation from other predicted changes. Warming of the oceans, decreasing oxygen levels (Gruber, 2011; Riebesell and Gattuso, 2015) and an OA induced reduction in the export of organic material to the deep ocean (reduced ballast effect – Codispoti, 2010; Gehlen et al., 2011) are all expected to impact on N_2O production and release to the atmosphere. Each of these conditions offers a positive feedback to a warming environment with regards their impacts on N_2O and so to a greater or lesser extent will counter the reduction in N_2O caused by OA. The individual stressors are identified but combined effects may prove to be additive, synergistic or antagonistic (Riebesell and Gattuso, 2015) and the ultimate impact of these multiple stressors in the ocean offers an unknown, uncharacterised and currently unpredictable control over the release of N_2O to the atmosphere.

Acknowledgments

This work was funded by NERC Grant UKOA-Ocean Acidification impacts on sea-surface, biology, biogeochemistry & climate (NE/H017259/1). We would like to thank Eric Acterberg, Richard Sanders and Mark Stinchcombe for nutrient measurements; Matthew Humphreys, Eithne Tynan and Mariana Ribas-Ribas for carbonate chemistry and Mark Moore and Sophie Richier for the management of bioassay manipulations and incubations. We are grateful to Steven Biller for providing the alignment of the *amoA* AOA sequences and to Tom Bell for discussions concerning the relationship between NH_3 and NH_4^+ .

Appendix A. Supplementary material

Supplementary data associated with this article can be found in the online version at <http://dx.doi.org/10.1016/j.dsr2.2015.12.006>.

References

- Bange, H.W., 2006. New directions: the importance of oceanic nitrous oxide emissions. *Atmos. Environ.* 40 (1), 198–199.
- Bell, T.G., Johnson, M.T., et al., 2007. Ammonia/ammonium dissociation coefficient in seawater: a significant numerical correction. *Environ. Chem.* 4 (3), 183–186.
- Bell, T.G., Johnson, M.T., et al., 2008. Ammonia/ammonium dissociation coefficient in seawater: a significant numerical correction. *Environ. Chem.* 5 (3), 258.
- Beman, J.M., Chow, C.-E., et al., 2011. Global declines in oceanic nitrification rates as a consequence of ocean acidification. *Proc. Natl. Acad. Sci. USA* 108 (1), 208–213.
- Biller, S.J., Mosier, A.C., et al., 2012. Global biodiversity of aquatic ammonia-oxidizing archaea is partitioned by habitat. *Front. Microbiol.* 3 (252). <http://dx.doi.org/10.3389/fmicb.2012.00252>.
- Bopp, L., Resplandy, L., et al., 2013. Multiple stressors of ocean ecosystems in the 21st century: projections with CMIP5 models. *Biogeosciences* 10 (10), 6225–6245.
- Borcard, D., Gilet, F., et al., 2011. *Numerical Ecology* with R. Springer, New York.
- Borowitzka, M.A., 1981. Photosynthesis and calcification in the articulated coralline red algae *Amphiroa-anceps* and *Amphiroa-foliacea*. *Mar. Biol.* 62 (1), 17–23.
- Bowen, J.L., Kearns, P.J., et al., 2013. Acidification alters the composition of ammonia-oxidizing microbial assemblages in marine mesocosms. *Mar. Ecol. Prog. Ser.* 492, 1–8.
- Bulow, S.E., Francis, C.A., et al., 2008. Sediment denitrifier community composition and *nirS* gene expression investigated with functional gene microarrays. *Environ. Microbiol.* 10 (11), 3057–3069.
- Ciais, P., Sabine, C., et al., Eds., 2013. Carbon and other biogeochemical cycles. *Climate change 2013: the physical science basis. Contribution of working group I to the fifth assessment report of the intergovernmental panel on climate change.* Cambridge University Press Cambridge, United Kingdom, New York, NY, USA.
- Clark, D.R., Brown, I.J., et al., 2014. The influence of ocean acidification on nitrogen regeneration and nitrous oxide production in the North-West European shelf sea. *Biogeosciences* 11, 4985–5005. <http://dx.doi.org/10.5194/bg-11-4985-2014>
- Codispoti, L.A., 2010. Interesting times for marine N_2O . *Science* 327 (5971), 1339–1340.
- Denman, K.L., Brasseur, G., et al., 2007. Couplings between changes in the climate system and biogeochemistry. *Climate change 2007: the physical science basis. Contribution of working group I to the fourth assessment report of the intergovernmental panel on climate change.* Solomon, S., Qin, D., Manning, M. et al., Cambridge, New York. pp. 499–587.
- Forster, G., Upstill-Goddard, R.C., et al., 2009. Nitrous oxide and methane in the Atlantic Ocean between 50 degrees N and 52 degrees S: Latitudinal distribution and sea-to-air flux. *Deep-Sea Res. Part II – Top. Stud. Oceanogr.* 56 (15), 964–976.
- Francis, C.A., Roberts, K.J., et al., 2005. Ubiquity and diversity of ammonia-oxidizing archaea in water columns and sediments of the ocean. *Proc. Natl. Acad. Sci. USA* 102 (41), 14683–14688.
- Freng, A., Wallace, D.W.R., et al., 2012. Global oceanic production of nitrous oxide. *Philos. Trans. R. Soc. B – Biol. Sci.* 367 (1593), 1245–1255.
- Fulweiler, R., Emery, H., et al., 2011. Assessing the role of pH in determining water column nitrification rates in a coastal system. *Estuaries Coasts* 34 (6), 1095–1102.
- Gattuso, J.-P., Magnan, A., et al., 2015. Contrasting futures for ocean and society from different anthropogenic CO_2 emissions scenarios. *Science* 349, 6243.
- Gattuso, J.P., Lavigne, H., 2009. Technical note: approaches and software tools to investigate the impact of ocean acidification. *Biogeosciences* 6 (10), 2121–2133.
- Gehlen, M., Gruber, N., et al., 2011. Biogeochemical consequences of ocean acidification and feedback to the earth system. In: Gattuso, J.P., Hansson, L. (Eds.), *Ocean Acidification*. Oxford University Press, Oxford, UK, pp. 230–248.
- Goreau, T.J., Kaplan, W.A., et al., 1980. Production of NO_2^- and N_2O by nitrifying bacteria at reduced concentrations of oxygen. *Appl. Environ. Microbiol.* 40, 526–532.
- Gruber, N., 2011. Warming up, turning sour, losing breath: ocean biogeochemistry under global change. *Philos. Trans. R. Soc. A – Math. Phys. Eng. Sci.* 369 (1943), 1980–1996.
- Hartmann, D.L., Tank, A.M.G.K., et al., 2013. Observations: atmosphere and surface. *Climate change 2013: the physical science basis. Contribution of working group I to the fifth.* In: Stocker, T.F., Qin, D., Plattner, G.-K., et al. (Eds.), assessment report of the intergovernmental panel on climate change. Cambridge University Press Cambridge, United Kingdom, New York, NY, USA.
- Hofmann, M., Schellnhuber, H.-J., 2009. Oceanic acidification affects marine carbon pump and triggers extended marine oxygen holes. *Proc. Natl. Acad. Sci. USA* 106 (9), 3017–3022. <http://dx.doi.org/10.1073/pnas.0813384106>.
- Huesemann, M.H., Skillman, A.D., et al., 2002. The inhibition of marine nitrification by ocean disposal of carbon dioxide. *Mar. Pollut. Bull.* 44 (2), 142–148.
- Hutchins, D.A., Fu, F.-X., et al., 2007. CO_2 control of trichodesmium N_2 fixation, photosynthesis, growth rates, and elemental ratios: implications for past, present, and future ocean biogeochemistry. *Limnol. Oceanogr.* 52 (4), 1293–1304.
- Hutchins, D.A., Mulholland, M.R., et al., 2009. Nutrient cycles and marine microbes in a CO_2 -enriched ocean. *Oceanography* 22 (4), 128–145.
- Kitidis, V., Laverock, B., et al., 2011. Impact of ocean acidification on benthic and water column ammonia oxidation. *Geophys. Res. Lett.* 38 (21), L21603.
- Kitidis, V., Upstill-Goddard, R.C., et al., 2010. Methane and nitrous oxide in surface water along the North-West Passage, Arctic Ocean. *Mar. Chem.* 121 (1–4), 80–86.
- Le Quéré, C., Peters, G.P., et al., 2014. Global carbon budget 2013. *Earth Syst. Sci. Data* 6 (1), 235–263.
- Lewis, E., Wallace, D.W.R., 1998. Program Developed for CO_2 System Calculations. Carbon Dioxide Information Analysis Center, Oak Ridge National Laboratory, U. S. Department of Energy, Oak Ridge, Tennessee, ORNL/CDIAC-105.
- Loescher, C.R., Kock, A., et al., 2012. Production of oceanic nitrous oxide by ammonia-oxidizing archaea. *Biogeosciences* 9 (7), 2419–2429.
- Moss, R.H., Edmonds, J.A., et al., 2010. The next generation of scenarios for climate change research and assessment. *Nature* 463 (7282), 747–756.
- Nevison, C.D., Weiss, R.F., et al., 1995. Global oceanic emissions of nitrous-oxide. *J. Geophys. Res.: Oceans* 100 (C8), 15809–15820.
- Ramaswamy, V., Boucher, O., et al., 2001. Radiative forcing of climate change. *Climate change 2001: the scientific basis. Contribution of working group I to the third assessment report of the intergovernmental panel on climate change.* In: Houghton, J.T., Ding, Y., Griggs, D.J., Noguer, M., Van der Linden, P.J., Dai, X., Maskell, K., Johnson, C.A., (Eds.) Cambridge University Press Cambridge, UK, pp. 349–416.
- Raven, J.A., Caldeira, K., et al., 2005. *Acidification Due to Increasing Carbon Dioxide.* The Royal Society, London.
- Ravishankara, A.R., Daniel, J.S., et al., 2009. Nitrous oxide (N_2O): the dominant ozone-depleting substance emitted in the 21st century. *Science* 326 (5949), 123–125.
- Rhein, M., Rintoul, S.R., et al., 2013. *Climate change 2013: the physical science basis. Contribution of working group I to the fifth assessment report of the intergovernmental panel on climate change.* Stocker, T.F., Qin, D., Plattner, G.-K., Tignor, M., Allen, S.K., Boschung, J., Nauels, A., Xia, Y., Bex, V., Midgley, P.M. Cambridge, United Kingdom, New York, USA.
- Riebesell, U., Gattuso, J.-P., 2015. Lessons learned from ocean acidification research. *Nat. Clim. Chang.* 5 (1), 12–14.
- Santorio, A.E., Buchwald, C., et al., 2011. Isotopic signature of N_2O produced by marine ammonia-oxidizing archaea. *Science* 333 (6047), 1282–1285.
- Santorio, A.E., Dupont, C.L., et al., 2015. Genomic and proteomic characterization of "Candidatus Nitrosopelagicus brevis": an ammonia-oxidizing archaeon from the open ocean. *Proc. Natl. Acad. Sci. USA* 112 (4), 1173–1178.
- Schulz, K.G., Barcelos e Ramos, J., et al., 2009. CO_2 perturbation experiments: similarities and differences between dissolved inorganic carbon and total alkalinity manipulations. *Biogeosciences* 6 (10), 2145–2153.
- Tynan, E., this issue.
- Tyrrell, T., Tarling, G.A., et al., this issue. Preface to special issue (Impacts of surface ocean acidification in polar seas and globally: a field-based approach).
- Upstill-Goddard, R.C., Rees, A.P., et al., 1996. Simultaneous high-precision measurements of methane and nitrous oxide in water and seawater by single phase equilibration gas chromatography. *Deep-Sea Res. Part I – Oceanogr. Res. Pap.* 43 (10), 1669–1682.
- Ward B.B., 2008a. Nitrification in marinmarine systems, In: D.G. Capone, D.A. Bronk, M.R. Mulholland and E.J. Carpenter (Eds.) *Nitrogen in the Marine Environment*, 2nd ed., Academic; Burlington, Massachusetts 199–261, <http://dx.doi.org/10.1016/B978-0-12-372522-6.00005-0>.
- Ward, B.B., 2008b. Phytoplankton community composition and gene expression of functional genes involved in carbon and nitrogen assimilation. *J. Phycol.* 44 (6), 1490–1503.
- Ward, B.B., Bouskill, N.J., 2011. The utility of functional gene arrays for assessing community composition, relative abundance, and distribution of ammonia-oxidising

- bacteria and archaea. *Methods Enzymol* 496, 373–396, Vol 46: Research on Nitrification and Related Processes, Pt B. M. G. Klotz and L. Y. Stein.
- Weiss, R.F., Price, B.A., 1980. Nitrous-oxide solubility in water and seawater. *Mar. Chem.* 8 (4), 347–359.
- Wuchter, C., Abbas, B., et al., 2006. Archaeal nitrification in the ocean. *Proc. Natl. Acad. Sci. USA* 103 (33), 12317–12322.
- Wyatt, N.J., Kitidis, V., et al., 2010. Effects of high CO₂ on the fixed nitrogen inventory of the Western English Channel. *J. Plankton Res.* 32 (5), 631–641.
- Zimmerman, G.M., Goetz, H., et al., 1985. Use of an improved statistical method for group comparisons to study effects of prairie fire. *Ecology* 66 (2), 606–611.